

Patterns of Vertical Root Fracture: Factors Affecting Stress Distribution in the Root Canal

Veera Lertchirakarn, MDSc, PhD, Joseph E. A. Palamara, PhD, and Harold H. Messer, MDSc, PhD

Previous studies have indicated that vertical root fracture tends to occur in a buccolingual direction, where dentin thickness is greatest. Factors potentially influencing the location and direction of root fracture include root canal shape, external root morphology, and dentin thickness. In this finite-element study, simulated root sections were varied systematically with respect to canal size and shape, external root morphology, and dentin thickness to determine their relative contribution to vertical root fracture. Similar models were constructed based on cross-sections of human tooth roots that had been fractured clinically or experimentally. Finite-element models demonstrated that canal curvature seems more important than external root morphology, in terms of stress concentration, and that reduced dentin thickness increases the magnitude but not the direction of maximum tensile stress. Models based on actual root fractures showed a strong similarity between tensile-stress distribution and fracture patterns.

Many studies, clinical (1, 2) and experimental (3–5), have been conducted to investigate patterns and causes of vertical root fracture (VRF). A consistent observation from these studies is a predominantly buccolingual direction of fracture regardless of the tooth or root involved, but the mechanism of fracture leading to this typical characteristic has not been clear. VRF is most commonly attributed to stresses generated within the canal during obturation (especially lateral condensation) or from a post placed in the canal (3–9). VRF in nonendodontically treated teeth also has been described (10), with characteristics similar to other forms of VRF.

Because the stresses predisposing to VRF are considered to be generated within the canal space, the pattern of stress distribution on the root canal surface is likely to be critical in directing crack initiation and fracture propagation. The measurement of stresses on the surface of the root canal, however, is not technically feasible. As shown previously (11), finite-element analysis (FEA) is a useful technique that can be used reliably in the analysis of stress distributions, with appropriate validation. Using models based on

actual tooth roots, nonuniform stress distributions were observed in cross-sections of the root. Regardless of whether the applied load was uniformly applied over the entire canal wall or at points simulating a spreader binding against the canal wall, tensile stresses were greatest on the buccal and lingual/palatal canal walls. The patterns of tensile-stress distribution closely matched observed distributions of VRF. The results of stress distribution in that study did not allow us to draw conclusions regarding which factors play the major role in creating nonuniform stress distribution.

Several studies have examined stress and strain distributions in root dentin using FEA (12, 13) but have not systematically evaluated the major factors that predispose to nonuniform stress distribution. The objectives of this FEA study were: (a) to compare quantitatively the tensile-stress distribution from various models of simulated canal sections; and (b) to relate stress patterns to fracture patterns observed in teeth subjected to clinical or experimental VRF. The combination of previous studies and these models should yield information regarding the factors that influence the nonuniformity of stress distribution in the mechanism of VRF.

MATERIALS AND METHODS

Development of Idealized Models of Root Dentin and Canal

Six simple models were developed, beginning with a radially symmetrical thick-walled cylinder with a dentin thickness of 1 mm and a central canal 1 mm in diameter. The models were then systematically varied by changing the cross-sectional shape of the canal (round or oval), the cross-sectional shape of the external root surface (round or oval), and the dentin thickness (Table 1). All models were 3 mm in height. These models were created using geometrical calculations to derive coordinates of the points on the inner (canal) and outer (root) surfaces of the cylinder.

CYLINDRICAL ROOT AND CANAL (MODEL I)

This dentin model was radially symmetrical, with 1 mm dentin thickness and a centrally located round canal 1 mm in diameter.

OVAL ROOT WITH ROUND CANAL (MODEL II)

The outer shape of this model was oval, but the inner (canal) space was circular with the same diameter (1 mm) as in the

TABLE 1. Summary of inner (root canal) and outer (root surface) shapes of dentin models, ratios of thickness of dentin, and the maximum tensile stresses on the root canal wall, as derived from 3-D FEA models

Model	Outer Root Shape	Inner (Canal) Shape	Ratio of Dentin Thickness (Buccolingual:Proximal)	Maximum Tensile Stress* (MPa)
I	circular	circular	1:1	1.27
II	oval	circular	1:0.5	1.82
III	circular	oval	1:1.25	2.24
IV	oval	oval	1:1	2.43
V	oval	oval	1:0.75	2.78
VI	oval	oval	1:0.5	3.50

* Derived from peak plot of specific area.

previous model. The thickness of the dentin wall varied from 1 mm in the thickest part (a notional buccolingual direction) to 0.5 mm in the thinnest part (a notional proximal direction).

CYLINDRICAL ROOT WITH OVAL CANAL (MODEL III)

The external root surface was round and the canal shape was oval, with a buccolingual canal diameter of 1 mm and a proximal diameter of 0.5 mm. As a result, dentin thickness ranged from 1 mm on the buccal and lingual aspects to 1.25 mm proximally.

OVAL ROOT WITH OVAL CANAL, AND VARYING DENTIN THICKNESS (MODELS IV–VI)

The internal canal shape was kept constant as in model III (buccolingual diameter 1 mm, proximal diameter 0.5 mm), whereas the thickness of proximal dentin was varied. Buccal and lingual dentin was constant at 1-mm thick, whereas proximal dentin was 1-mm (model IV), 0.75-mm (model V), or 0.5-mm (model VI) thick.

Development of Models Based on Fractured Roots

Simple root models were developed from two teeth that fractured asymmetrically in clinical function or from a previous experimental study (5) by digitizing a single cross-section of each root at the level of the VRF. The models included only periodontal ligament (PDL) and a 1 mm thickness of root length in the area of interest.

MANDIBULAR INCISOR (MODEL VII)

This model was created from a tooth used in our previous study (5). The root was kidney-shaped in cross-section, with a single oval canal. Buccolingual dentin thickness was approximately double the mesiodistal thickness. The fracture line was in a buccolingual direction but tangential to the canal surface rather than through the middle of the canal.

MAXILLARY PREMOLAR (MODEL VIII)

The model was created from a clinical case of VRF related to a large post in the palatal canal. The fracture pattern was complex, with two fracture lines on the palatal surface of the root and a third fracture line on the buccal surface, with the fracture passing through both canals.

Selection of the Element Types

Eight-node hexahedral elements and a small percentage of six-node pentahedral elements were chosen. Each idealized dentin model consisted of 384 elements and 600 nodes. Each fractured root model consisted of 768 elements and 1080 nodes in the structure. The properties of dentin and other tissues were as described in the previous study (11).

Applied Load and Boundary Conditions

SIMPLE DENTIN MODELS (I–VI)

A structural face load of 1 N was applied to each model in a perpendicular direction around the surface of the canal. This loading represented a uniform distribution of circumferential stress. The boundary conditions (support) of these models, constrained in x, y, and z directions, were fixed at the external lower surface of the models.

FRACTURED TOOTH ROOTS (MODELS VII, VIII)

A structural face load of 60 N was applied to points on the canal surface that were contacted by the spreader or the post, based on tracings from the cross-sectional views of each tooth. Loading was perpendicular to canal surfaces. The boundaries were constrained in x, y, and z directions at the entire external periodontal ligament. The remaining nodes were given 3 degrees of freedom.

Analysis

Linear elastic isotropic analysis was used as in the previous study (11). The analysis of these FEA models was focused on the patterns of tensile-stress distribution throughout the thickness of root dentin from the inner (canal) wall to the outer root surface. Stress contour plots provided a graphical representation of the stress variation in a mid-level cross-section of each model. The maximum tensile stress of each model also was computed.

RESULTS

As in the previous study (11), only tensile stresses are presented. The magnitudes of stresses were compared quantitatively among simple dentin models because of the similar geometry and loading conditions. Results are qualitative for the fractured roots because

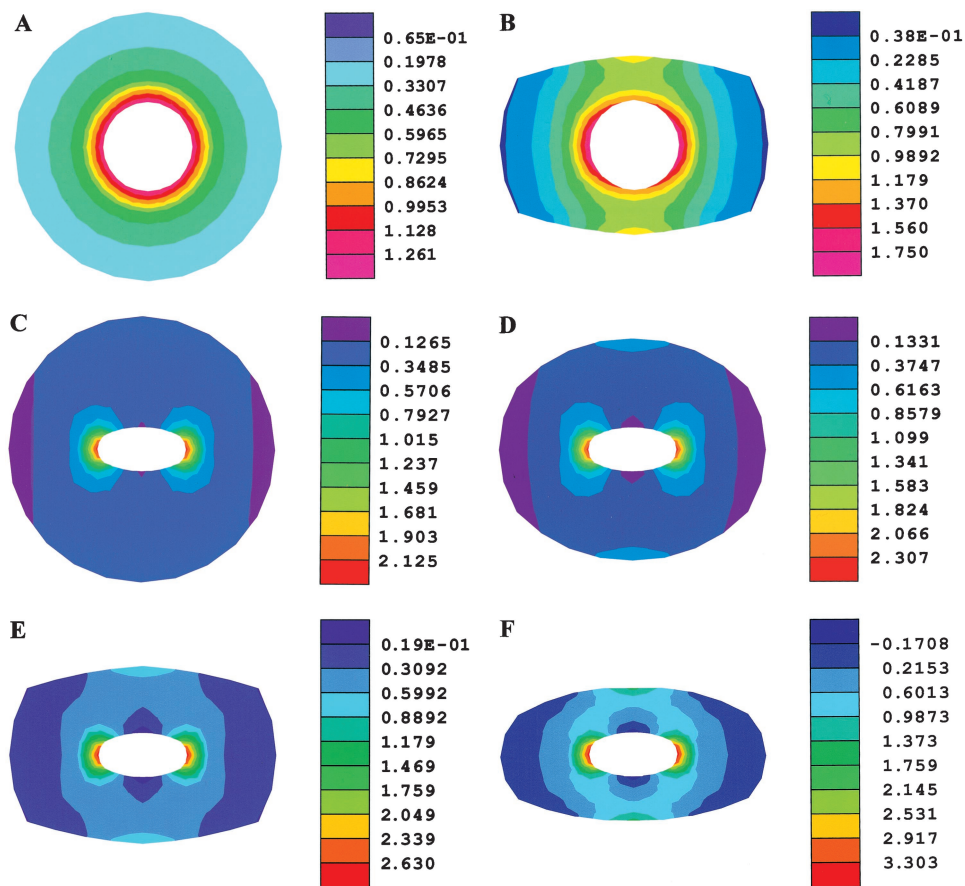


Fig 1. (A–F) Stress contours of model I (A), model II (B), model III (C), model IV (D), model V (E), and model VI (F), showing stress distribution of tensile (S1) stress. Each color represents a range of stress values (in MPa) corresponding to the scale.

the distribution of stresses in relation to fracture pattern was considered the most important comparison.

Simple Dentin Models

Overall, tensile stresses were greatest on the inner (canal) surface and lowest on the outer (root) surface. Stresses were radially symmetrical in the simple cylindrical model as expected, and declined progressively from the inner surface to the outer surface. A change in the cross-sectional shape of the canal or root surfaces resulted in an asymmetrical stress distribution. Tensile stress was elevated on the canal wall in the direction of the increased canal or root curvature (i.e. in a notional buccal and lingual direction).

MODEL I

A symmetrical tensile-stress gradient was observed from the canal to the root surface. The maximum tensile stress was located at the internal surface with a value of 1.26 MPa (Fig. 1A).

MODEL II

Reduction of proximal dentinal thickness by 50% by changing the outer root profile from round to oval (with a round canal) resulted in an elevated maximum tensile stress, to 1.82 MPa.

Greatest stresses were in the buccolingual direction where dentin thickness was greatest. This model also showed higher tensile stress on the outer proximal surface than on the buccal and lingual surfaces (Fig. 1B).

MODEL III

When the canal shape was oval but the outer profile was round, the highest tensile stress was 2.24 MPa, with a strong concentration of stresses at the points of maximum canal curvature (buccal and lingual aspects). Proximal dentin thickness was greatest in this model (1.25 mm), and greater than on the buccal and lingual aspects (1.0 mm) (Fig. 1C).

MODELS IV TO VI

When both the inner and outer surface profiles were oval, tensile stresses were again concentrated on the buccal and lingual canal surfaces and were much lower on the proximal canal surfaces. As the proximal dentin thickness decreased, the magnitude of the maximal tensile stress increased but the distribution remained unchanged (Fig. 1, D to F). Maximum tensile stress on the buccal and lingual canal walls increased from 2.43 MPa, when dentin thickness was uniformly 1.0 mm, to 3.50 MPa, when proximal dentin thickness was 0.5 mm (Table 1).

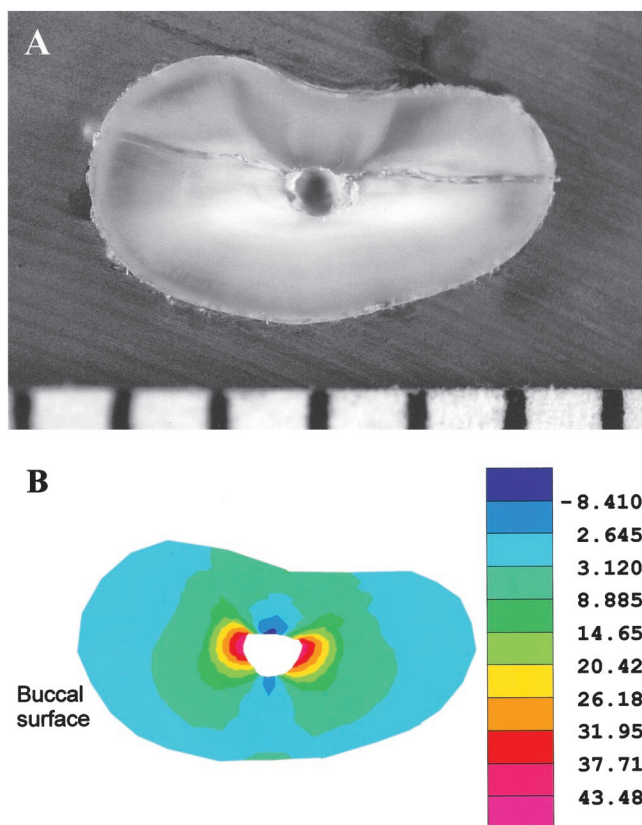


FIG 2. (A) Cross-section of a mandibular incisor root fractured 5 mm from the root apex, showing the irregular root shape and fracture lines deviating from the middle of the canal in a buccolingual direction (the scale is 1 mm). (B) Tensile-stress contours (S1) from a model of the fractured root (model VII). The cross-sectional view depicts tensile-stress distributions, which also deviated toward the concave aspect of the root, although still in a predominantly buccolingual direction. Each color represents a range of stress values (in MPa) corresponding to the scale.

Fractured Tooth Roots

MODEL VII (IRREGULAR MANDIBULAR INCISOR ROOT)

This root showed a predominantly buccolingual fracture, but the fracture line was almost tangential to the proximal canal wall rather than passing through the middle of the canal (Fig. 2A). The FEA model showed the highest tensile stresses at the canal wall, decreasing toward the root surface. Tensile stresses were oriented predominantly in a buccolingual direction, but with maximum tensile-stress concentrations inclined toward the concave proximal root surface (Fig. 2B). Thus the tensile-stress distribution mimicked the fracture pattern.

MODEL VIII (MAXILLARY PREMOLAR ROOT WITH POST, FRACTURED IN CLINICAL FUNCTION)

The cross-section of the root showed a complex fracture pattern, with two oblique fracture lines on the palatal surface of the root inclined mesially and distally, and a third fracture line on the buccal surface (Fig. 3A). The fracture line passed through both canals, and the post appeared to contact most of the palatal wall of the palatal canal. The FEA model also showed an asymmetrical

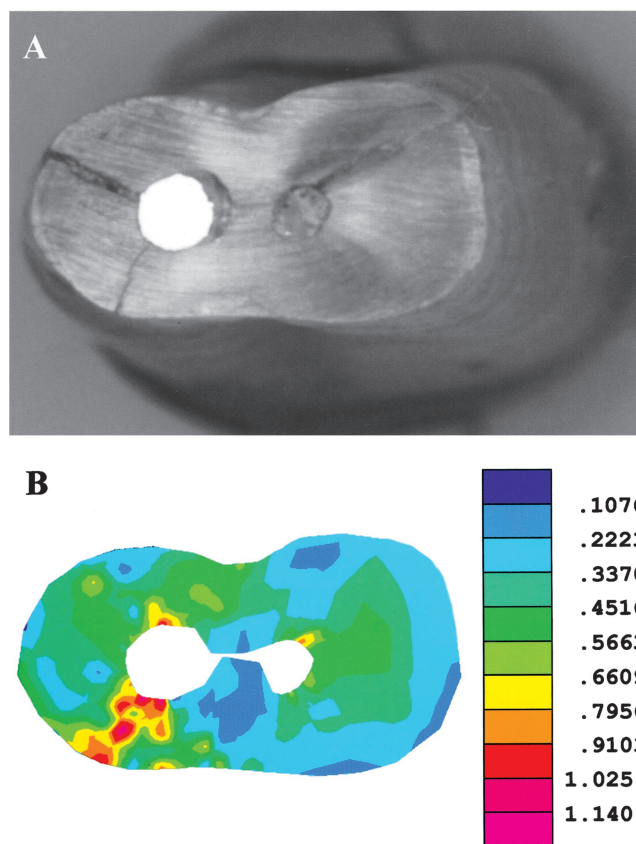


FIG 3. (A) Cross-section of a clinical vertical root fracture of a maxillary premolar with post, 5 mm from the root apex, showing the contact area of post and root canal wall and fracture lines. (B) Tensile-stress contours (S1) of the fractured root (model VIII). Each color represents a range of stress values (in MPa) corresponding to the scale.

tensile-stress distribution predominantly in a buccolingual direction, with highest stresses on the root canal surface (Fig. 3B). The localized high tensile-stress concentrations coincided approximately with the clinical fracture lines.

DISCUSSION

This study sought to explain why the nonuniform tensile-stress distribution is in a predominantly buccolingual direction, although dentin is thicker in this direction than in the mesiodistal direction. The study also investigated which factors play the greatest roles in stress distribution. This information should provide a better understanding of VRF behavior.

A series of FEA models was constructed, beginning with a simple, thick-walled cylinder with little resemblance to any human tooth root (with the possible exception of maxillary central incisors or distal roots of mandibular molars). With the progressive changes in inner and outer surface shapes and the reduction in proximal dentin thickness, the final model resembled an idealized, single-canal, mandibular incisor. All stresses were generated on the inner wall, consistent with stresses occurring during obturation or post preparation and placement (1, 3–5, 11).

The simple, radially symmetrical thick-walled cylinder (model I, control) showed the predicted symmetrical stress distribution, with circumferential tensile stress decreasing from the inner to the

outer surface (Fig. 3A). This stress distribution follows the basic pattern of hoop stresses in a thick-walled cylindrical pressure vessel (14). Rupture would occur only when the tensile strength of dentin was exceeded, and could occur in any location around the dentin wall. Any localized region of stress concentration would predispose to crack initiation at that location (15).

When the inner or outer surface of the model was changed to an oval shape, or the wall thickness was reduced in one direction, stress distribution was no longer uniform. Reducing the radius of curvature of the inner (canal) wall or outer root surface resulted in an increased tensile stress on the inner wall, in the same direction as the location of the reduced radius of curvature. A decreased radius of curvature of both inner and outer walls had a strong impact on stress distribution, which was further accentuated by a reduction in wall thickness on the "proximal" surfaces. A consistent feature of all of the asymmetrical models, however, was the increased tensile-stress concentrations in the notional buccolingual direction, regardless of the thickness of the proximal dentin wall. In fact, progressively reducing proximal dentin thickness resulted in an increased buccolingual stress concentration, further predisposing to buccolingual fracture. In all of these models, crack initiation would occur on the buccal or lingual canal surface and propagate to the outer root surface (15). This pattern is consistent with the clinical and experimental observations of buccolingual fractures occurring through the thickest part of dentin (1, 5, 8, 11). In numerous cross-sections of human teeth, we have noted that the greatest thickness of dentin tends to occur at sites of lowest radius of curvature of the canal; in mandibular incisors, dentin thickness in a buccolingual direction is often double that of proximal dentin (11).

In these models, decreasing proximal dentin thickness increased the tendency for buccolingual stress concentration and hence the predisposition to buccolingual fracture. This pattern is counter-intuitive; most people would predict fracture through the thinnest part of dentin. When pressure is applied in a thick-walled vessel, stresses in the wall are of two types: tensile stress in a circumferential direction; and compressive stress in a radial direction (14). The thin part of the wall will be forced to expand more readily than the thick part of the wall in a radial direction. The asymmetrical expansion creates additional circumferential tensile stresses on the inner surface of the thicker areas, resulting from the outward bending of the thinner part of the dentin wall.

All of the three factors investigated (canal shape, root shape, and dentin thickness) affected tensile-stress distribution, with interactions among all three factors. Canal shape seemed to be the single most important factor, with a reduced radius of curvature strongly influencing stress concentration (15). Changing the outer root shape from round to oval, with a round canal (model II), resulted in a smaller increase in maximum tensile stress than changing the inner canal shape from round to oval (model III) (Table 1). The highest stress concentrations occurred when both inner and outer shapes were oval. The effect of dentin thickness was the reverse of what might have been predicted (16), with greater stress buccolingually as proximal dentin thickness was reduced. A comparison of models V and II (Fig. 1, B and E), which have the same external root shape, shows that changing the canal shape from oval to round actually relieves internal stresses despite the substantial thinning of proximal dentin. A markedly oval root shape is more susceptible to high stress than a more circular one. However, the root with a combination of the three factors is the most susceptible to VRF, such as mandibular incisors and mesial roots of mandibular molars.

Natural teeth will have the additional factor of localized irregularities in canal or outer root morphology, which may lead to even greater stress concentrations. Two fractured roots were modeled, showing asymmetrical root fracture. The mandibular incisor showed a decided concavity on the distal root surface, and the path of fracture was eccentric: buccolingual in overall direction but toward the side of the canal closest to the root concavity. The FEA model showed that tensile stresses were highest in inner dentin and concentrated buccolingually, but with a subtle inclination toward the distal (concave) root surface. The maxillary premolar, fractured clinically after a large post was cemented in the palatal canal, showed highest stress concentrations toward the mesiopalatal and distopalatal line angles, with a third area of stress concentration in the buccal canal. In both cases, a strong similarity between modeled stress and fracture patterns was observed, with localized irregularities in the canal wall resulting in specific areas of stress concentration. This coincided with previous clinical (1, 2, 6–8) and experimental (3, 4, 9, 17, 18) reports of characteristic patterns of VRF. This result implies that the irregularity of the root canal also affects the stress distribution and VRF.

The results from the previous report (11) and this study provide a basis for better understanding the behavior of VRF and how to prevent it. Localized stresses in inner dentin are most closely associated with VRF. These stresses may occur during or after endodontic treatment, when the tooth is subjected to occlusal force or further clinical procedures such as post placement. Thus, decreasing the applied force during endodontic or restorative procedures (obturation, post placement) is significant in reducing the risk of fracture, especially in teeth such as mandibular incisors and lower molars, which are susceptible to VRF.

Mechanical instrumentation of root canals can produce craze lines on the root canal wall (16), which may serve as localized sites of increased stress (in accordance with stress-concentration theory). Instrumentation procedures should be undertaken with gentle force and using copious irrigation to minimize crazing. The dentist's goal should be to create a root canal shape that maximizes radius of curvature of the root canal wall. A circular shape minimizes stress concentration areas and will distribute stress more uniformly. Furthermore, procedural errors that create stress concentration areas on the root canal wall, such as ledging, gouging, crazing, etc., should be avoided. Although canal cross-sectional shape seems more important than dentin thickness in stress distribution, removal of root dentin should be minimized. By maintaining dentin thickness as much as possible, especially in the proximal areas or in the thin part of root dentin, additional stress from bending mechanisms will be minimized. Caution has to be exercised in any procedure involving a tooth that is susceptible to VRF.

This study was supported by a grant from the National Health and Medical Research Council of Australia.

Dr. Lertchirakarn was a former postgraduate student, School of Dental Science, University of Melbourne. He is a lecturer, Department of Operative Dentistry, Faculty of Dentistry, Chulalongkorn University, Thailand. Dr. Palamara is lecturer, and Dr. Messer is professor of Restorative Dentistry, School of Dental Science, University of Melbourne, Victoria, Australia.

Address requests for reprints to Harold H. Messer, School of Dental Science, University of Melbourne, 711 Elizabeth Street, Melbourne 3000, Australia.

References

1. Walton RE, Michelich RJ, Smith GN. The histopathogenesis of vertical root fractures. *J Endodon* 1984;10:48–56.
2. Selden HS. Repair of incomplete vertical root fractures in endodontically treated teeth—In vivo trials. *J Endodon* 1996;22:426–9.
3. Holcomb JQ, Pitts DL, Nicholls JI. Further investigation of spreader loads required to cause vertical root fracture during lateral condensation. *J Endodon* 1987;13:277–84.
4. Saw LH, Messer HH. Root strains associated with different obturation techniques. *J Endodon* 1995;21:314–20.
5. Lertchirakarn V, Palamara JEA, Messer HH. Load and strain during lateral condensation and vertical root fracture. *J Endodon* 1999;25:99–104.
6. Tamse A. Iatrogenic vertical root fractures in endodontically treated teeth. *Endod Dent Traumatol* 1988;4:190–6.
7. Wechsler SM, Vogel RI, Fishelberg G, Shovlin FE. Iatrogenic root fractures: a case report. *J Endodon* 1978;4:251–3.
8. Meister F, Lommel TJ, Gerstein H. Diagnosis and possible causes of vertical root fractures. *Oral Surg* 1980;49:243–53.
9. Pitts DL, Matheny HE, Nicholls JI. An in vitro study of spreader loads required to cause vertical root fracture during lateral condensation. *J Endodon* 1983;9:544–50.
10. Chan CP, Tseng SC, Lin CP, Huang CC, Tsai TP, Chen CC. Vertical root fracture in nonendodontically treated teeth: a clinical report of 64 cases in Chinese patients. *J Endodon* 1998;24:678–81.
11. Lertchirakarn V, Palamara JEA, Messer HH. Finite element analysis and strain gauge studies of vertical root fracture. *J Endodon* (in press).
12. Ricks-Williamson LJ, Fotos PG, Goel VK, Spivey JD, Rivera EM, Khera SC. A three-dimensional finite-element stress analysis of an endodontically prepared maxillary central incisor. *J Endodon* 1995;21:362–7.
13. Yaman SD, Alaçam T, Yaman Y. Analysis of stress distribution in a vertically condensed maxillary central incisor root canal. *J Endodon* 1995;21:321–5.
14. Muvdi BB, McNabb JW. Selected topics. In: *Engineering mechanics of materials*. 3rd ed. New York: Springer-Verlag, 1991:590–630.
15. Callister WD. Failure chapter. In: *Materials science and engineering: an introduction*. 4th ed. New York: John Wiley & Sons, Inc., 1997:178–228.
16. Wilcox LR, Roskelley C, Sutton T. The relationship of root canal enlargement to finger spreader induced vertical root fracture. *J Endodon* 1997;23:533–4.
17. Murgel CAF, Walton RE. Vertical root fracture and dentin deformation in curved roots: the influence of spreader design. *Endod Dent Traumatol* 1990;6:273–8.
18. Monaghan P, Bajalcaliev JG, Kaminski EJ, Lautenschlager EP. A method for producing experimental simple vertical root fractures in dog teeth. *J Endodon* 1993;19:512–5.